Biosensors and Bioelectronics 31 (2012) 445–450

Contents lists available at SciVerse ScienceDirect

Biosensors and Bioelectronics

journal homepage: www.elsevier.com/locate/bios

Ca^{2+} ion transport through channels formed by α-hemolysin analyzed using a microwell array on a Si substrate

Koji Sumitomo[a,*], Arianna McAllister[a,1], Yukihiro Tamba[b], Yoshiaki Kashimura[a], Aya Tanaka[a], Youichi Shinozaki[a,2], Keiichi Torimitsu[a]

[a] NTT Basic Research Laboratories, NTT Corporation, 3-1 Morinosato Wakamiya, Atsugi, Kanagawa 243-0198, Japan
[b] Suzuka National College of Technology, Shiroko-cho, Suzuka, Mie 510-0294, Japan

ARTICLE INFO

Article history:
Received 14 October 2011
Accepted 6 November 2011
Available online 15 November 2011

Keywords:
Nano-biodevices
Ion channels
Artificial lipid bilayer
Suspended lipid bilayer
Microwell array

ABSTRACT

For the functional analysis of ion channel activity, an artificial lipid bilayer suspended over microwells was formed that ruptured giant unilamellar vesicles on a Si substrate. Ca^{2+} ion indicators (fluo-4) were confined in the microwells by sealing the microwells with a lipid bilayer. An overhang formed at the microwells prevented the lipid membrane from falling into them and allowed the stable confinement of the fluorescent probes. The transport of Ca^{2+} ions through the channels formed by α-hemolysin inserted in a lipid membrane was analyzed by employing the fluorescence intensity change of fluo-4 in the microwells. The microwell volume was very small (1–100 fl), so a highly sensitive monitor could be realized. The detection limit is several tens of ions/s/μm^2, and this is much smaller than the ion current in a standard electrophysiological measurement. Smaller microwells will make it possible to mimic a local ion concentration change in the cells, although the signal to noise ratio must be further improved for the functional analysis of a single channel. We demonstrated that a microwell array with confined fluorescent probes sealed by a lipid bilayer could constitute a basic component of a highly sensitive biosensor array that works with functional membrane proteins. This array will allow us to realize high throughput and parallel testing devices.

1. Introduction

Supported artificial lipid bilayers have attracted attention because of their potential for device applications as well as their fundamental scientific interest (Bayley and Cremer, 2001; Janshoff and Steinem, 2006; Sackmann, 1996). For biodevices that work with functional membrane proteins such as ion channels, a lipid bilayer is a key material as regards protein functions (Bally et al., 2010). Major barriers to fabricating a biodevice using membrane proteins are the creation of stable lipid bilayers, guaranteeing protein activity, and the detection of their functions. To overcome these barriers, various lipid bilayer formation and structural geometries have been investigated as well as supported lipid bilayers. These include black lipid membranes (Ide and Yanagida, 1999; Ide et al., 2002; Pantoja et al., 2001; Römer and Steinem, 2004; Winterhalter, 2000), tethered bilayer membranes on solid surfaces (Keizer et al., 2007; Raguse et al., 1998; Terrettaz et al., 2003), and lipid bilayers suspended over nanostructures (Cheng et al., 2001; Favro et al., 2002; Sumitomo et al., 2010). In particular, the combination of biological systems and semiconductor nanotechnology offers great potential for device applications (Kleefen et al., 2010; Hemmler et al., 2005; Rahman et al., 2005; Römer et al., 2004; Shinozaki et al., 2010; Sumitomo et al., 2009, 2010).

In our previous study, we succeeded in confining fluorescent probes in a microwell array by sealing the array with lipid bilayers (Sumitomo et al., 2010). A lipid bilayer suspended over the microwells was formed by rupturing giant unilamellar vesicles (GUVs) on a substrate. The use of GUVs avoids the formation of multiple lipid bilayers and guarantees the formation of a single lipid bilayer. In addition, the obtained lipid bilayer is free from any organic solvents that may affect the function of the membrane proteins. The modification of the microwell apertures prevents the lipid bilayer from falling into the microwells and its stability is greatly enhanced. Therefore, the probability of the successful confinement of fluorescent probes in the microwells is sufficiently improved. It is possible to seal many microwells with a lipid bilayer by rupturing a single GUV, and so we can fabricate a device array that measures the ion channel function. In addition, the leakage of the fluorescent probes

* Corresponding author. Tel.: +81 46 240 3457; fax: +81 46 270 2364.
E-mail address: sumitomo.koji@lab.ntt.co.jp (K. Sumitomo).
[1] Present address: University of Toronto, 5 King's College Road, Toronto, ON M5S 3G8, Canada.
[2] Present address: University of Yamanashi, 1110 Shimokato, Chuo, Yamanashi 409-3898, Japan.

0956-5663/$ – see front matter © 2011 Elsevier B.V. All rights reserved.
doi:10.1016/j.bios.2011.11.010

confined in the microwells is negligible. A microwell array with fluorescent probes has the potential for analyzing the ion channel activity of membrane proteins.

In this work, we investigated the activity of an α-hemolysin ion channel using an array of microwells on a Si substrate. α-Hemolysin is a bacterial exotoxin with a membrane-damaging function and its structure and function have been widely studied (Fang et al., 1997; Menestrina et al., 2001; Noskov et al., 2004; Song et al., 1996). The cytotoxic property of α-hemolysin is mediated by the formation of a pore in the cell membrane. α-Hemolysin monomers are inserted into the lipid membrane and then oligomerized to form a heptameric transmembrane pore, thus providing a good prototype for the analysis of transmembrane pores and ion channels. The transport of Ca^{2+} ions was studied by analyzing the fluorescence intensity of a Ca^{2+} ion indicator (fluo-4) confined in microwells on a Si substrate. And, we demonstrate that an array of microwells sealed with lipid bilayers is a powerful tool for the functional analysis of membrane proteins, and will become a basic component of nano-biodevices that work with functional proteins.

2. Material and methods

2.1. Microwell chips

A microwell pattern on a Si substrate covered with a 120-nm thick thermal oxide layer was fabricated using a conventional photolithographic and dry etching technique. The microwells were circular with diameters of 1, 2, 4, or 8 μm, and were 1 μm deep. An overhang shape was formed at the microwell apertures by selective etching (Seidel et al., 1990; Williams and Muller, 1996) with KOH (10 wt.%) for 15 min after removing the native oxide from inside the microwells by treating them with NH_4F for 3 min. The shapes of the microwells were confirmed by using scanning electron microscopy (SEM), as shown in Fig. 1a and b. The Si substrate under the SiO_2 overlayer was selectively etched and {1 1 1} facets appeared. A cross-sectional SEM image (Fig. 1b), which was measured after using a focused ion beam (FIB) to cut along the dashed line in Fig. 1a, clearly shows that the remaining SiO_2 layer forms an overhang. The maximum length of the overhang was estimated to be approximately 1 μm. The modification of the microwell structure promotes the confinement of fluorescent probes and buffer in the microwells as well as the formation of suspended lipid bilayers, as shown in Fig. 1c (Sumitomo et al., 2010). The surface roughness of SiO_2 after the process was completed was estimated to be less than 0.3 nm (RMS) from AFM images measured in air.

2.2. Materials

The lipids 1,2-diphytanoyl-sn-glycero-3-phosphocholine (DPhPC), 1,2-dipalmitoyl-sn-glycero-3-phosphoethanolamine-N-(lissamine rhodamine B sulfonyl) (Rhod-DPPE), and cholesterol were obtained from Avanti Polar Lipids (Alabaster, AL). Ca^{2+} ion indicator fluo-4 was purchased from Invitrogen (Carlsbad, CA). EDTA was purchased from Nacalai Tesque (Kyoto, Japan).

Lyophilized powder of α-hemolysin from *Staphylococcus aureus* was purchased from Sigma–Aldrich (St. Louis, MO). α-Hemolysin was dissolved in PBS at a concentration of 5 mg/ml, and was stored at −20 °C in a freezer. Stock solution was diluted by PBS to 0.05–0.5 mg/ml just before use.

2.3. Formation of GUVs

The GUVs were prepared by the electroformation method (Dimitrov and Angelova, 1988). DPhPC and cholesterol were dissolved in chloroform up to a final concentration of 2.5 mM, and then combined to a final molar ratio of 8:2 DPhPC:Chol. Rhod-DPPE was used at 1 mol% as a dye for labeling the lipid bilayers. A chloroform solution of lipid was spread evenly on an ITO-coated glass slide. The slide was dried in a vacuum for 2 h, and then a chamber was constructed from a lipid-coated slide and an uncoated slide coupled

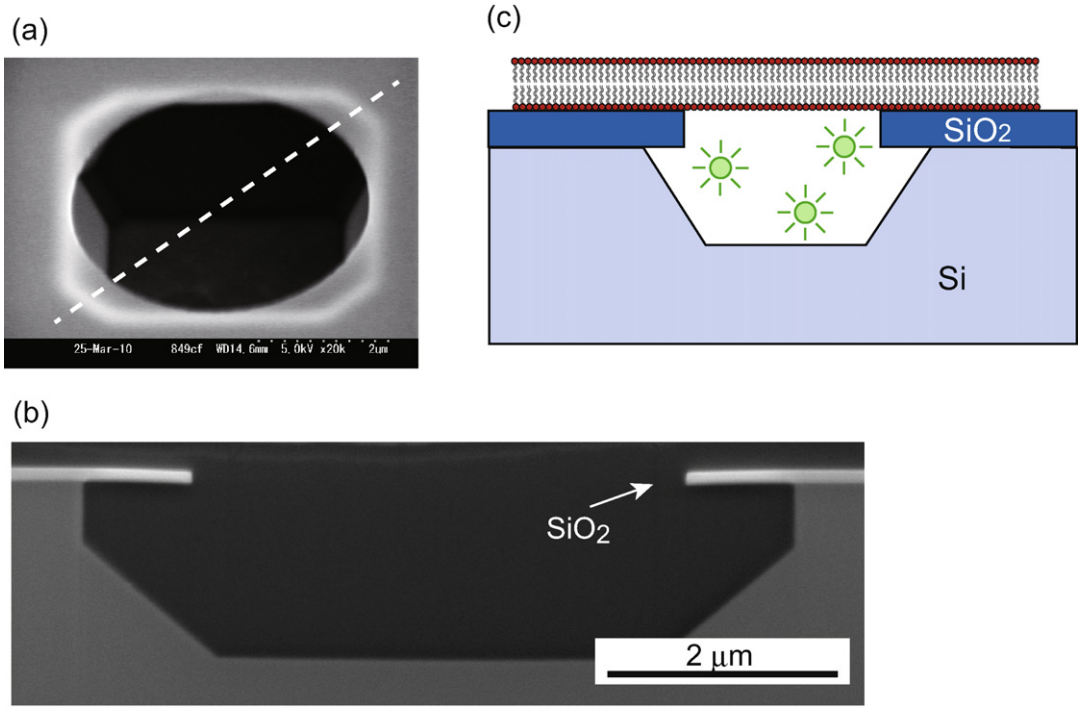

Fig. 1. (a) Typical SEM image of microwells on a Si substrate. The microwell aperture is 4 μm in diameter. The image was obtained with a 5-keV electron beam and its tilt angle was 45°. (b) Cross-sectional SEM image of the microwells along the dashed line in (a). (c) Schematic illustration of the confinement of fluorescent probes in the microwells achieved by sealing them with a lipid bilayer.

with 1-mm thick silicon rubber. The chamber was filled with sucrose solution (200 mM). The GUVs were grown by supplying an AC voltage of 1 V at 10 Hz for 2 h while heating the chamber to 60 °C.

2.4. Confinement of fluo-4 in microwells

A lipid bilayer suspended over microwells was formed by rupturing the GUVs (Hamai et al., 2007). A mixture of glucose solution (160 mM), NaCl (20 mM), a Ca^{2+} indicator (10 μM of fluo-4), and EDTA (1 mM) was placed on the substrate and the microwells were filled with the solution. Several μl of GUV suspension were added to the glucose solution on the substrate, and the GUVs slowly sank onto the substrate surface. After incubation for 10 min, almost all the GUVs ruptured on the substrate. The fluo-4 was confined in the microwells by sealing them with lipid bilayers. The excess fluo-4 outside the microwells was rinsed off with glucose solution (160 mM) containing NaCl (20 mM).

2.5. Confocal laser scanning microscope

The samples were observed with a confocal laser scanning microscope BX51-FV300 (Olympus Ltd., Japan) under a 40× objective lens. We used laser light sources emitting at 488 and 543 nm for excitation, and 505–525 nm band-pass filters and high-pass filters of over 610 nm to detect the fluorescence from fluo-4 and Rhod-DPPE, respectively. The stability of fluorescence intensity from fluo-4 confined in the microwells was confirmed as shown in Fig. S1. The laser power was set to minimize the effect of photobleaching, and the leakage of fluo-4 was negligible.

3. Results and discussion

3.1. Fluorescence intensity change induced by Ca^{2+} ion transport

By rupturing GUVs, the fluo-4 was confined in the microwells in a glucose solution (160 mM) with NaCl (20 mM). Then, to analyze the Ca^{2+} ion transport through the ion channels, a difference was realized between the Ca^{2+} ion concentrations of the microwells and the outer solution by adding $CaCl_2$ to the outer solution until its concentration reached 1 mM. Fluorescence microscope observation was initiated after waiting for 150 s until the Ca^{2+} ion concentration in the outer solution became uniform. Time lapse images were captured at 3 s intervals, and the transport of the Ca^{2+} ions from the outer solution to inside the microwells was investigated in terms of the fluorescence of the fluo-4 confined in the microwells. Thirty seconds after the start of the measurement, 20 μl of α-hemolysin (0.1 mg/ml) was added. The final concentration of the α-hemolysin in the outer solution was 200 nM. Fig. 2a–f shows fluorescence images for 488-nm excitation obtained after 0, 5, 6, 7, 10, and 15 min, respectively, and Fig. 2g shows the fluorescence from a rhodamine-B labeling lipid patch observed with 543-nm excitation. Even over the microwells, the bright fluorescence of rhodamine-B from the suspended lipid bilayer was observed. Almost all the microwells except those close to the edge of the lipid patch were successfully sealed by the lipid bilayer. Only the two microwells indicated by the white arrows in Fig. 2g were not sealed.

The fluo-4 in several microwells began to fluoresce 5 min after the start of the measurement as shown in Fig. 2b. The fluorescence intensity of the fluo-4 increased for several minutes, and a bright emission was observed from all the microwells sealed by the lipid bilayer at 7 min (Fig. 2d). This indicates that the Ca^{2+} ions were transported from the outer solution to inside the microwells through ion channels formed by α-hemolysins. Fig. 3 shows the change in fluorescence intensity as a function of the elapsed time from the fluo-4 confined in the microwells labeled A, B, C, and D shown in the inset. The fluorescence intensity began to increase several minutes after the α-hemolysin was added to the outer solution. A few minutes were needed for the diffusion of the α-hemolysin molecules in the solution, the insertion of the molecules into the lipid bilayer suspended over the microwells, and the assembly of seven molecules to form the ion channel. The onset time of the change in the fluorescence intensity has a

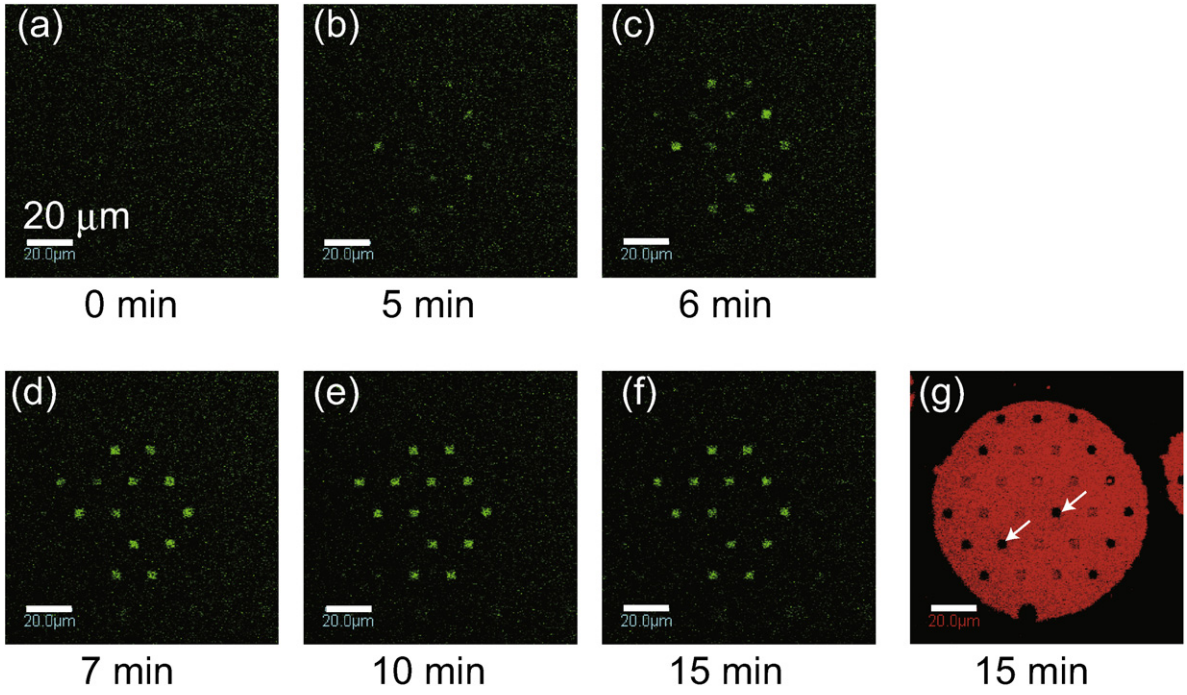

Fig. 2. Fluorescent microscope images of the microwells with 4 μm diameter apertures sealed with a lipid bilayer. (a)–(f) The fluorescence from fluo-4 confined in the microwells was measured by 488 nm excitation at 0, 5, 6, 7, 10, and 15 min, respectively, using time-lapse imaging. (g) The fluorescence from rhodamine-B conjugated with lipid (543 nm excitation) shows a circular patch of lipid bilayer over the microwells.

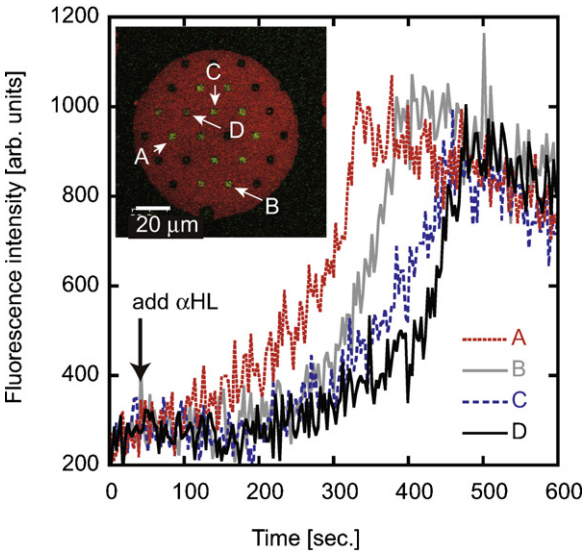

Fig. 3. Change in fluorescence intensity from fluo-4 confined in the microwells as a function of elapsed time. The inset shows a fluorescence microscope image of microwells A, B, C, and D.

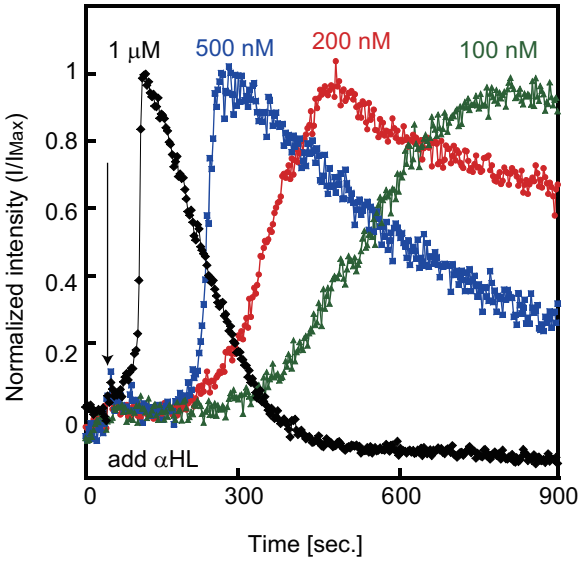

Fig. 4. Change in fluorescence intensity induced by the addition of various concentrations of α-hemolysin. α-Hemolysin with a final concentration of 1 μM, 500 nM, 200 nM, or 100 nM was added 30 s (arrow in the figure) after the beginning of time-lapse imaging.

wide distribution because these processes are not uniform. There is a difference of 2 min between the onset times of the change for an early microwell (A) and a late microwell (D). The state of the increasing intensity also differs depending on the wells. For example, microwells (B), (C) and (D) are similar as regards the time at which the increase in the fluorescence intensity began. The intensity of microwell (B) increased quickly and reached its maximum value at 400 s. On the other hand, the intensity of microwell (D) increased slowly until 450 s and subsequently became quicker. An increase in the rate of the intensity change indicates an increase in the number of ion channels formed with α-hemolysin.

The insertion of α-hemolysin in a suspended lipid membrane and the formation of nanopores induces the transport of Ca^{2+} ions, and the fluorescence intensity of fluo-4 increased as a result. When the α-hemolysin concentration is higher, the fluorescence intensity should reach its maximum value earlier. The changes in the fluorescence intensity of the fluo-4 contained in the microwells are plotted as a function of time in Fig. 4 for various α-hemolysin concentrations. PBS (20 μl) with various α-hemolysin concentrations was added 30 s after starting the fluorescent microscope observation. The fluorescence intensity was normalized by dividing it by the maximum intensity after subtracting the background, namely the fluorescence intensity before adding α-hemolysin. When 1 μM (final concentration) α-hemolysin was added, the concentration reached its maximum value only 80 s after the addition. This was only about 10 s after an increase of fluorescence intensity was observed. The permeability became large, because a large number of α-hemolysin molecules were inserted into the lipid membrane suspended over the microwells and many channels were formed. The fluorescence intensity also began to increase earlier. This indicates that the probability of assembling α-hemolysin molecules to form a transmembrane pore is also high because of the high density of the molecules in the lipid membrane. The leakage of Ca^{2+} ions through the lipid bilayer or/and the water layer between the lipid bilayer and the substrate was not negligible but not very serious as shown in Fig. S2. A change in the fluorescence intensity caused by the α-hemolysin concentration shows clearly that Ca^{2+} ions penetrate the channels formed by α-hemolysin, not a water layer.

After the fluorescence intensity reached its maximum value, it gradually decreased. Under these experimental conditions, the effect of photobleaching is not very serious, as shown in Fig. S1. This indicates that the fluorescent probes (fluo-4) as well as the Ca^{2+} ions were able to pass through the channel. The minimum diameter of an ion channel formed by α-hemolysin is only 1.5 nm (Song et al., 1996), but this is sufficient for the transportation of fluo-4, whose molecular weight is 927.

3.2. Transport rate of Ca^{2+} ion through α-hemolysin channel

The rate of the increase in fluorescence intensity indicating Ca^{2+} ion transport and the rate of decrease ($-dI/dt$) indicating fluo-4 leakage are plotted as a function of the α-hemolysin concentration in Fig. 5a and b, respectively. Each rate was measured at $I/I_{max} = 0.5$ during the fluorescence intensity change, and the transport ratios of ions were estimated as follows. The fluorescence intensity is almost saturated at 10 μM Ca^{2+} ions, because the binding coefficient of fluo-4 with Ca^{2+} ions is sufficiently high (Gee et al., 2000). The fluorescence intensity increases as well as the Ca^{2+} ion concentration at a low concentration sufficiently below saturation, but when the fluorescence intensity approaches saturation, the linear relation disappears. Therefore, we analyzed the ion transport using the fluorescence intensity change at half the maximum intensity by assuming that there is a linear relation between fluorescence intensity and Ca^{2+} ion concentration.

In addition, some fluo-4 leaked out through the channel formed by α-hemolysin until the fluorescence intensity reached its maximum value. However, the increase in the fluorescence intensity caused by the transport of Ca^{2+} ions is almost 20 times faster than the decrease caused by the leakage of fluo-4. Therefore, the fluo-4 leak was ignored in the analysis of Ca^{2+} ion transport. The relation between the normalized fluorescence intensity I and the Ca^{2+} ion concentration in the microwells, C_{Ca}, was assumed to be as follows for the low Ca^{2+} ion concentration region.

$$C_{Ca} = C_{sat} I[\mathrm{M}] \quad (C_{Ca} < C_{sat}) \tag{1}$$

Here, $C_{sat} = 10 \times 10^{-6}$ [M], which is the Ca^{2+} ion concentration for the saturation of the fluorescence intensity. Therefore, the flux of

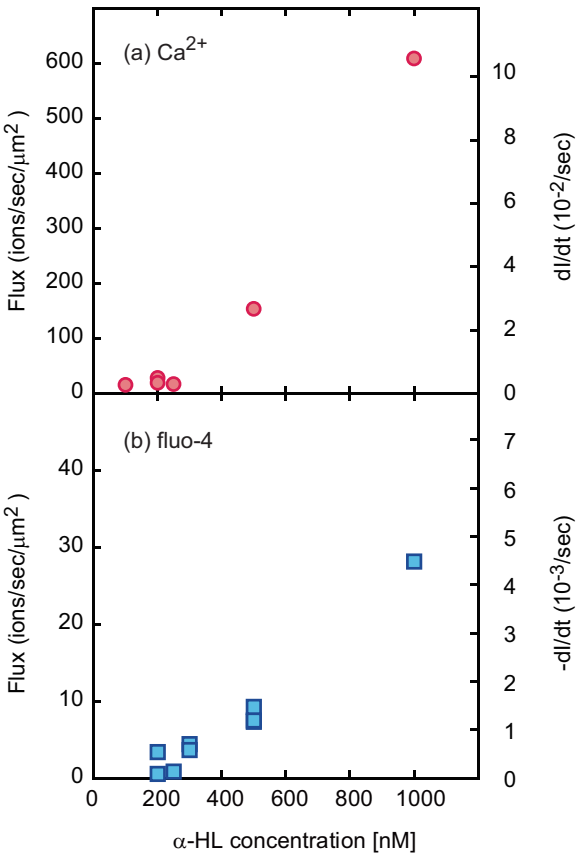

Fig. 5. (a) Transport ratio of Ca^{2+} ions through the channels as a function of the α-hemolysin concentration. It was estimated from the value of dI/dt at $I/I_{max} = 0.5$. (b) Transport ratio of fluo-4 leakage through the channels.

the Ca^{2+} ions, J_{Ca}, is calculated by Eq. (2) and plotted as a function of α-hemolysin concentration in Fig. 5a.

$$J_{Ca} = C_{sat} N_A \frac{V}{S} \left(\frac{dI}{dt}\right) \quad (\text{ions/s/}\mu\text{m}^2) \tag{2}$$

Here, N_A is Avogadro's number, V is the volume of microwells, and S is the effective area of the lipid membrane suspended over the microwells. For all the microwells with different diameters used in this study, the ratio (V/S) of the volume to the effective area corresponds to the microwell depth ($d = 1\ \mu m$). A small V/S value for the microwells results in a large change in the ion concentration even when the flux of the Ca^{2+} ions (J_{Ca}) is small.

After the fluorescence intensity reaches its maximum value, it decreases with the leakage of fluo-4 through the channel. Since the initial fluo-4 concentration (C_{init}) in the microwells is 10 mM, the flux of fluo-4 is estimated as follows and $J_{fluo\text{-}4}$ is plotted in Fig. 5b.

$$J_{fluo\text{-}4} = C_{init} N_A \frac{V}{S} \left(\frac{-dI}{dt}\right) \quad (\text{ions/s/}\mu\text{m}^2) \tag{3}$$

The transport of the Ca^{2+} ions and fluo-4 depends on the number of channels, which is decided by the α-hemolysin concentration. When there was less than 200 nM of α-hemolysin, very few channels were formed. Since seven molecules of α-hemolysin should be aggregated to form a channel, we need an α-hemolysin concentration that exceeds a certain threshold. The flux of the Ca^{2+} ions (J_{Ca}) and fluo-4 ($J_{fluo\text{-}4}$) increased with a rise of the α-hemolysin concentration, when 200 nM or more α-hemolysin was added. Fig. 5a shows the successful detection of Ca^{2+} ion transport through α-hemolysin channels with high sensitivity as the detection limit is several ten ions/s/μm^2. For the transport of fluo-4, a very slow leak of a few ions/s/μm^2 was detected (Fig. 5b). The Ca^{2+} ion detection limit is closely related to the leakage of Ca^{2+} ions through the lipid bilayer and/or the water layer between the lipid bilayer and the substrate (Fig. S2). The lipid bilayer suspended over the microwells is stable enough for the measurement of Ca^{2+} ion transport as shown in Fig. S3.

The higher transport of the Ca^{2+} ions compared with that of fluo-4 is induced by the fact that the Ca^{2+} ion gradient is higher than that of fluo-4 at the lipid bilayer. The Ca^{2+} ions moved spontaneously down their concentration gradient from outside (initial concentration: 1 mM) to inside (initial concentration: 0 mM) the microwells. On the other hand, the difference between the inside and outside fluo-4 concentrations in the microwells was only 10 μM. When considering the concentration gradient, it should be noted that the permeability of fluo-4 is somewhat larger than that of Ca^{2+} ions. The effect of an electric charge and the reactivity with the inside of the channels formed by α-hemolysin seem to reduce the permeability of Ca^{2+}. In a standard electrophysiological measurement, we measured a pA order electric current under an electric bias of around 100 mV. However, no external electric field was supplied in this analysis. The ion transport was driven simply by the ion concentration gradient. The ion transport observed in this experiment was four or five orders smaller than that obtained with a standard

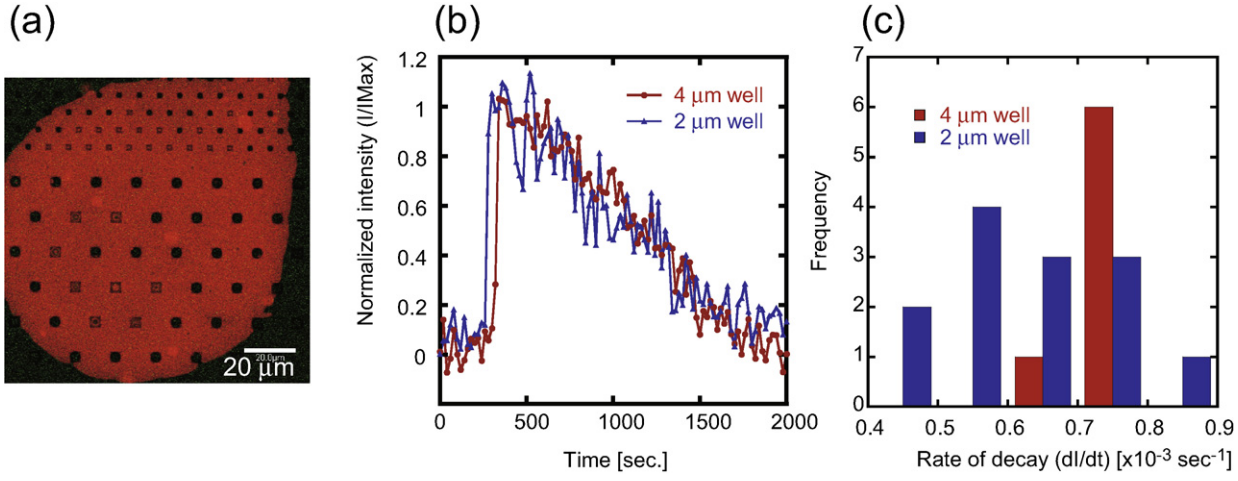

Fig. 6. (a) A fluorescent microscope image of a lipid patch sealing 2 and 4 μm microwells. (b) Change in fluorescence intensity induced by forming channels with α-hemolysin (final concentration 300 nM). (c) Distribution of decay rate for each microwell.

electrophysiological measurement. Moreover, it is also possible to use this device to detect other types of ions in addition to Ca^{2+} ions by using other types of ion indicators. If we choose the excitation and emission wavelengths of the ion indicators appropriately, we can also expect to measure more than one ion at the same time.

To investigate the effect of microwell size, 2-μm and 4-μm microwells were sealed simultaneously with a single patch as shown in Fig. 6a. This lipid patch sealed seven 4-μm microwells and thirteen 2-μm microwells. Since the microwell depth is constant, the volume of the 2-μm microwells is one quarter that of the 4-μm microwells. However, the curves of the fluorescence intensity changes for 4- and 2-μm microwells are almost the same, as shown in Fig. 6b. The distribution of the decay rate of the fluorescence intensity caused by the transport of fluo-4 is shown in Fig. 6c. The average rates $(-dI/dt)$ are 0.72 ± 0.02 and 0.63 ± 0.04 $(\times 10^{-3}/\mathrm{s})$ for the 4- and 2-μm microwells, respectively. These rates correspond to 54 and 12 molecules/s for the transport ratio of fluo-4 per microwell. The fluorescence intensity change of the fluo-4 in the microwells is independent of microwell size. In other words, the number of ions transported through the ion channels is largely proportional to the area of the microwells. This indicates that more than one channel was formed and the number is proportional to the effective area of the lipid membrane. Smaller microwells will make it possible to mimic a local ion concentration change in the cells, although the signal to noise ratio must be further improved for the functional analysis of a single channel.

4. Conclusion

We succeeded in monitoring Ca^{2+} ion transport through channels formed by α-hemolysin using microwells sealed with artificial lipid membranes. The small microwell volume results in a big change in the ion concentration even when the ion permeation is small. The detection limit for Ca^{2+} transport was estimated to be several tens of ions/s/μm^2. We demonstrated that an array of microwells sealed by a lipid membrane can act as a highly sensitive sensor array. Such microwell arrays are promising components for nano-biodevices for the functional analysis of ion channel-type membrane proteins, and they will enable the fabrication of high throughput and parallel testing devices.

Acknowledgments

We thank Tooru Morimitsu for his experimental support throughout this research. This research was supported in part by a Grant-in-Aid for Scientific Research B20360014 from the Japan Society for the Promotion of Science (JSPS).

Appendix A. Supplementary data

Supplementary data associated with this article can be found, in the online version, at doi:10.1016/j.bios.2011.11.010.

References

Bally, M., Bailey, K., Sugihara, K., Grieshaber, D., Vörös, J., Städler, B., 2010. Small 22, 2481–2497.
Bayley, H., Cremer, P.S., 2001. Nature 413, 226–230.
Cheng, Y., Bushby, R.J., Evans, S.D., Knowles, P.F., Miles, R.E., Ogier, S.D., 2001. Langmuir 17, 1240–1242.
Dimitrov, D.S., Angelova, M.I., 1988. Bioelectrochem. Bioenerg. 19, 323–336.
Fang, Y., Cheley, S., Bayley, H., Yang, J., 1997. Biochemistry 36, 9518–9522.
Favro, G., D'Annibale, A., Campanella, L., Santucci, R., Ferri, T., 2002. Anal. Chim. Acta 460, 23–34.
Gee, K.R., Brown, K.A., Chen, W-N.U., Bishop-Stewart, J., Gray, D., Johnson, I., 2000. Cell Calcium 27, 97–106.
Hamai, C., Cremer, P.S., Musser, S.M., 2007. Biophys. J. 92, 1988–1999.
Hemmler, R., Böse, G., Wagner, R., Peters, R., 2005. Biophys. J. 88, 4000–4007.
Ide, T., Takeuchi, Y., Yanagida, T., 2002. Single Mol. 3, 33–42.
Ide, T., Yanagida, T., 1999. Biochem. Biophys. Res. Commun. 265, 595–599.
Janshoff, A., Steinem, C., 2006. Anal. Bioanal. Chem. 385, 433–451.
Keizer, H.M., Dorvel, B.R., Andersson, M., Fine, D., Price, R.B., Long, J.R., Dodabalapur, A., Köper, I., Knoll, W., Anderson, P.A.V., Duran, R.S., 2007. Chembiochem 8, 1246–1250.
Kleefen, A., Pedone, D., Grunwald, C., Wei, R., Firnkes, M., Abstreter, G., Rant, U., Tampe, R., 2010. Nano Lett. 10, 5080–5087.
Menestrina, G., Serra, M.D., Prévost, G., 2001. Toxicon 39, 1661–1672.
Noskov, S.Y., Roux, W., Im, B., 2004. Biophys. J. 87, 2299–2309.
Pantoja, R., Sigg, D., Blunck, R., Bezanilla, F., 2001. Biophys. J. 81, 2389–2394.
Rahman, Md.M., Nonogaki, Y., Tero, R., Kim, Y.-H., Uno, H., Zhang, Z.-L., Yano, T., Aoyama, M., Sasaki, R., Nagai, H., Yoshida, M., Urisu, T., 2005. Jpn. J. Appl. Phys. 44, L1207–L1210.
Raguse, B., Braach-Maksvytis, V., Cornell, B.A., King, L.G., Osman, P.D.J., Pace, R.J., Wieczorek, L., 1998. Langmuir 14, 648–659.
Römer, W., Lam, Y.H., Fisher, D., Watts, A., Fischer, W.B., Göring, P., Wehrspohn, R.B., Gösele, U., Steinem, C., 2004. J. Am. Chem. Soc. 126, 16267–16274.
Römer, W., Steinem, C., 2004. Biophys. J. 86, 955–959.
Sackmann, E., 1996. Science 271, 43–48.
Seidel, H., Csepregi, L., Heuberger, A., Baumgärtel, H., 1990. J. Electrochem. Soc. 137, 3612–3626.
Shinozaki, Y., Sumitomo, K., Furukawa, K., Miyashita, H., Tamba, Y., Kasai, N., Nakashima, H., Torimitsu, K., 2010. Appl. Phys. Express 3, 027002.
Song, L., Hobaugh, M.R., Shustak, C., Cheley, S., Bayley, H., Gouaux, J.E., 1996. Science 274, 1859–1866.
Sumitomo, K., Shinozaki, Y., Takagi, D., Nakashima, H., Kobayashi, Y., Torimitsu, K., 2009. Jpn. J. Appl. Phys. 48, 08JB18.
Sumitomo, K., Tamba, Y., Shinozaki, Y., Torimitsu, K., 2010. Appl. Phys. Express 3, 107001.
Terrettaz, S., Mayer, M., Vogel, H., 2003. Langmuir 19, 5567–5569.
Williams, K.R., Muller, R.S., 1996. J. Microelectrochem. Syst. 5, 256–269.
Winterhalter, M., 2000. Curr. Opin. Colloid Interface Sci. 5, 250–255.